Directional imaging of the retinal cone mosaic

Brian Vohnsen, Ignacio Iglesias, and Pablo Artal

Laboratorio de Óptica, Universidad de Murcia, Campus de Espinardo (Edificio C), 30071 Murcia, Spain

Received November 20, 2003

We describe a near-IR scanning laser ophthalmoscope that allows the retinal cone mosaic to be imaged in the human eye *in vivo* without the use of wave-front correction techniques. The method takes advantage of the highly directional quality of cone photoreceptors that permits efficient coupling of light to individual cones and subsequent detection of most directional components of the backscattered light produced by the light-guiding effect of the cones. We discuss details of the system and describe cone-mosaic images obtained under different conditions. © 2004 Optical Society of America

OCIS codes: 170.4470, 170.5810, 330.5310.

The fundus of the living human eye is routinely imaged either by flood illumination photography or with a scanning laser ophthalmoscope[1] (SLO) to reveal clinically relevant information about blood-vessel distribution, size of the optic disk, etc. In recent years the retinal cone mosaic has been resolved in living human eyes by high-resolution flood illumination systems[2–4] and by confocal SLOs.[5,6] To accomplish this imaging, both techniques have typically relied on the incorporation of adaptive optics to reduce the blurring caused by aberrations of the eye. The improvement in image resolution has therefore often been accompanied by an increase in system complexity and cost. Other, less-direct methods have also been proposed for high-resolution retinal imaging. These include methods based on speckle interferometry[7] and on the deconvolution of ocular aberrations from images obtained with flood illumination.[8]

We propose here a technique based on the directionality of the cone photoreceptors. It is well known that the cones are well aligned[9,10] and have light-guiding properties similar to those of optical fibers.[11] These properties are manifested by the Stiles–Crawford effect, viz., reduced visual sensitivity to light that is incident off axis onto the eye's pupil.[12] Thus light that intersects any given cone photoreceptor at an angle is substantially diminished in visual response because of reduced coupling efficiency. These cone properties are also responsible for a corresponding directional component in light scattered back from the retina.[13–15] In this Letter we report on a novel SLO technique for retinal cone-mosaic imaging that takes advantage of the strong directional component in light scattered from the retina. This directional light exits the eye through a small fraction of the entire pupil area[14] and therefore suffers little from aberrations. As a consequence, the incorporation of wave-front correction techniques may not be as necessary as in previous imaging techniques.

Figure 1 is a schematic of the confocal SLO that we use, together with diagrams of the underlying imaging principle involved. Scanning is done by two galvanometric mirror scanners, one of which is operated at resonance, that allow 512×512 pixel-sized images to be recorded at an ~15-Hz frame rate. We previously described a similar system in combination with adaptive optics.[16] A near-IR ($\lambda = 0.785\ \mu$m) collimated laser beam with ~3-mm spot size is incident upon the pupil, whose center functions as pivot point for raster scanning. The beam is truncated to ~2 mm, resulting in an increased signal for the same illumination power. This phenomenon can be understood in terms of the Stiles–Crawford effect and of a reduced influence of ocular aberrations. The expected size of the focused spot (~6 μm for an ideal diffraction-limited eye) suffices to expose single cones or a small number of cones at the periphery of the foveal region, assuming a hexagonal arrangement with ~11-μm spacing and ~10,000 cones/mm^2 as a typical cone density.[17] The light that returns from the fundus is collimated by the optics of the eye and descanned, and an image of the illuminated region is formed in the plane of the confocal pinhole. In the system the transverse magnification from retina to pinhole plane is 4×. The pinhole serves to enhance the relative contribution of directional light from the cones to the signal by discriminating against

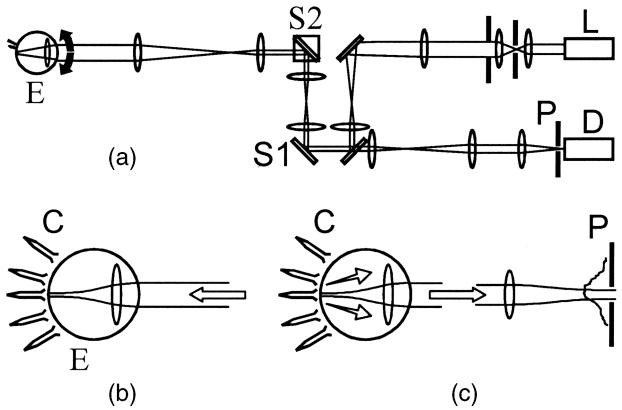

Fig. 1. (a) Schematic of the confocal SLO used for imaging of the eye's fundus (E), including L, a laser diode; S1 resonant and S2 nonresonant galvanometric mirror scanners; P, confocal pinhole; and D, a photomultiplier tube for detection. Below are diagrams that illustrate the underlying imaging principle: (b) the incoming scanning beam coupled to a single (or a few) cone photoreceptors (C) and (c) the corresponding light returned from the retina that contains guided in addition to scattered components that are imaged in the plane of the pinhole.

0146-9592/04/090968-03$15.00/0

light scattered from other retinal structures and elsewhere. This can be done because scattered light, in general, suffer aberrations when it leaves the eye through a large dark-adapted pupil (~6 mm exit pupil) and is therefore poorly focused in the plane of the pinhole. In consequence, it contributes little to the signal unless wave-front correction techniques are implemented.[6] The key point in our approach is therefore to select a pinhole that is sufficiently small to facilitate the capture of directional light from cones while it blocks unwanted scattered light from blurring image detail. A photomultiplier tube with internal amplification and voltage conversion for an improved signal-to-noise ratio is used to measure the optical signal, and a maximum of 15 consecutive frames are collected and stored in a PC with a 20-MHz digital oscilloscope for subsequent imaging. In the results presented, all frames have been corrected for the distortion produced by the harmonic motion of the resonant scanner, and 6–8 subsequent frames of each image have been correlated and averaged numerically to improve the signal-to-noise ratio.

Retinal images of the right eye of one of the authors (BV: 34 years old, normal vision) with different pinholes are shown in Fig. 2. Results similar to those shown have been obtained from the eyes of other subjects. In all cases the incident light's power was kept at (or below) 150 μW, which is ~4× less than the safety standard for continuous exposure in the small-source limit.[18] A gradual improvement in resolution with decreasing pinhole size is apparent from Figs. 2(c)–2(f). The larger pinholes give the stronger signal but also more blur of the retinal details, whereas the smaller pinholes produce images that clearly reveal the underlying cone mosaic, although they produce a weaker signal because of the rejection of a larger part of scattered light. We found that a ⌀30-μm pinhole (corresponding to ~7.5 μm at the retina) most effectively resolves the individual cones at this retinal location. All features do not appear to be equally bright in the images, a result that may reflect differences in the coupling efficiency caused by factors such as disorientation or misalignment of cones with respect to the incoming beam and variations in the mode field diameter that can be efficiently excited in each. It should be noted that the tiny blood vessels appear dark because they overlie the cones and thus (apart from absorption losses) perturb the coupling of light to the cones. Nevertheless, some cones can still be distinguished through the vessels, as may happen when the distortion of the incoming beam is small. The dark feature seen at the left borders of images 2(a) and 2(b) is the shadow produced by a LED used as a fixation target for the eye during imaging; the differently sized bright spots, aligned just above the area marked by a square in Fig. 2(a), are due to reflections in the system optics between scanners and eye. The influence of these reflections, however, is minor once the images are recorded with a smaller pinhole as in Fig. 2(b).

We have imaged the retina at various eccentricities to obtain information about the average cone spacing. Sections of such images were Fourier transformed, and the resultant average spectra are shown in Fig. 3 together with their radial profiles for two locations. A ringlike structure appears near the center of the spectral image, indicating a dominant radial frequency component that is representative of the cone spacing.[19] Its actual value can be read from the radial spectrum, where a peak at ~16 cycles/deg, corresponding to a spatial distance of ~17 μm, represents the approximate spacing between observed cone photoreceptors at ~1° eccentricity, whereas at a larger eccentricity of ~7° the peak is slightly shifted to ~14 cycles/deg, corresponding to a spatial distance of ~20 μm. As is apparent from the figure, however, these numbers are only approximate. Both peaks in the radial spectra are oscillating and broad, extending up to frequencies of ~34 cycles/deg, corresponding to ~8.2 μm, i.e., approximately the resolution limit imposed by the size of the pinhole. This spectral extension may partly explain the deviation of ~11 μm from the aforementioned value for the cone spacing based on data of Curcio *et al.*[17] Eye motion within each frame may also affect the image correlation and thus the estimated cone spacing by enhancing mostly lower frequencies. Unfortunately, the expected increment in cone density at small eccentricities cannot be seen clearly from our data. The chosen power limitation hinders the usage of a smaller pinhole as required to

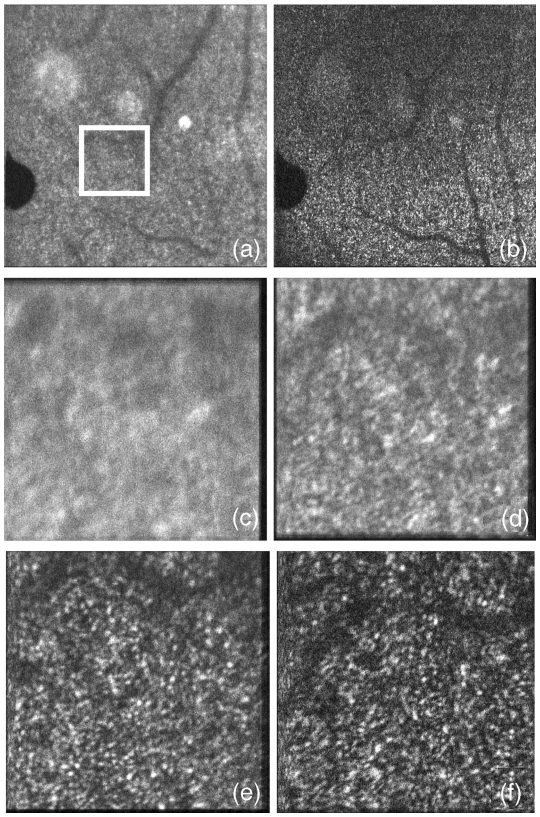

Fig. 2. Retinal images (a), (b) 8° × 8° and (c)–(f) 2° × 2° obtained with various sizes of the confocal pinhole: (a), (c) ⌀200, (d) ⌀100, and (e) ⌀50 μm and (b), (f) ⌀30 μm. The square in (a) indicates the area imaged in (c)–(f). Images (a) and (b) are centered at ~4° from the central fovea in the nasal direction. The average signal (normalized) is (a) 1.00, (b) ~0.04, (c) ~0.94, (d) ~0.32, (e) ~0.10, (f) ~0.04.

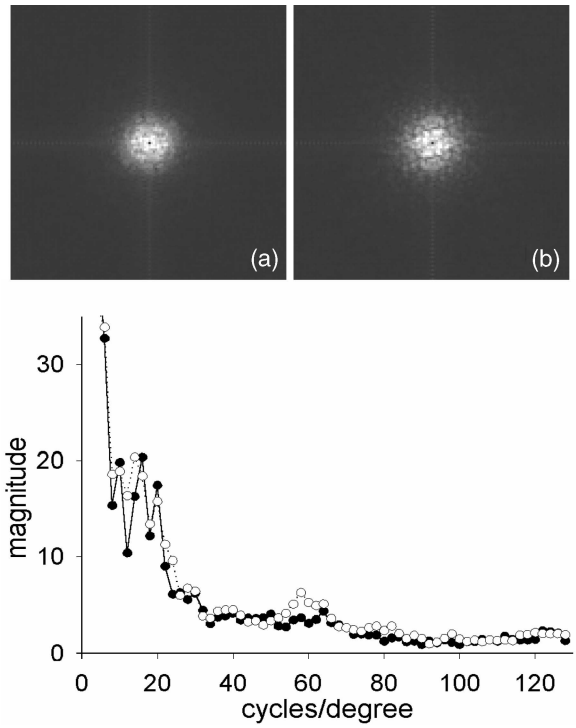

Fig. 3. Top, two-dimensional Fourier spectra at retinal eccentricities of (a) ~1° and (b) ~7° in the nasal direction. Bottom, corresponding radial Fourier spectra at the same retinal locations of ~1° (filled circles and solid curve) and ~7° (open circles and dotted curve). Each spectrum is an average of 10 calculated from similar sections of 2° × 2° images. The dc component has been set to zero.

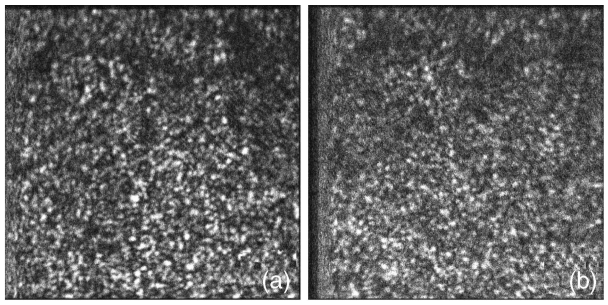

Fig. 4. Retinal images 2° × 2° obtained at different depths of the retina by axial displacement of the ⌀30-μm pinhole. It has been displaced by (a) 5 and (b) 10 mm toward the eye compared with the image in Fig. 2(f), corresponding to ~300 and ~600 μm, respectively, at the retina.

make cone-resolved imaging nearer the central fovea. A second broad peak in the radial spectrum can be distinguished at ~60 cycles/deg, corresponding to a spatial distance of ~4.7 μm. This is the observed mode field diameter and thus the apparent width of the cones.

Inasmuch as the system is selective to directional components of light, it shows essentially no depth-resolving capabilities. Thus the cone mosaic remains visible at widely different positions of the confocal pinhole, as shown in Fig. 4. The main consequence of axial displacement of the pinhole away from its optimal location is a reduction of the image contrast. This is an important advantage of the proposed technique because, even in the presence of some defocus or remnant aberrations, imaging of the cone mosaic remains possible.

In summary, we have demonstrated a technique based on a scanning laser ophthalmoscope optimized for imaging of the directional components of light returned from cone photoreceptors and shown that the technique can be used to resolve the retinal cone mosaic at the periphery of the foveal region. As mostly directional components contribute to image formation, the technique shows little depth selectivity, which facilitates the adjustment of the confocal pinhole but makes the imaging of retinal structures, other than cone mosaic and blood vessels, difficult. A larger signal, obtained by either improved optics or a better detection system, could potentially allow cone-resolved imaging nearer the central fovea, where the packing density is largest. Because of its ease of use the method may prove a suitable alternative to other techniques that are used for studying retinal cone spacing and directionality.

This research has been supported by the Spanish Fondo de Investigación Sanitaria (grants FIS 01/1463 and red IM3 G03/185) and the Ministerio de Ciencia y Tecnología (grant BFM2001-0391) and by a Marie-Curie fellowship HPMD-CT-2000-00052. B. Vohnsen's e-mail address is vohnsen@um.es.

References

1. R. H. Webb, G. W. Hughes, and O. Pomerantzeff, Appl. Opt. **19,** 2991 (1980).
2. J. Liang, D. R. Williams, and D. T. Miller, J. Opt. Soc. Am. A **14,** 2884 (1997).
3. A. Roorda and D. R. Williams, Nature **397,** 520 (1999).
4. F. Vargas-Martín, P. M. Prieto, and P. Artal, J. Opt. Soc. Am. A **15,** 2552 (1998).
5. A. R. Wade and F. W. Fitzke, Lasers Light **8,** 129 (1998).
6. A. Roorda, F. Romero–Borja, W. J. Donnelly III, H. Queener, T. J. Hebert, and M. C. W. Campbell, Opt. Express **10,** 405 (2002), http://opticsexpress.org.
7. P. Artal and R. Navarro, Opt. Lett. **14,** 1098 (1989).
8. I. Iglesias and P. Artal, Opt. Lett. **25,** 1804 (2000).
9. G. J. van Blokland, Vision Res. **26,** 495 (1986).
10. S. A. Burns, S. Wu, F. Delori, and A. Elsner, J. Opt. Soc. Am. A **12,** 2329 (1995).
11. J. M. Enoch, J. Opt. Soc. Am. **53,** 71 (1963).
12. W. S. Stiles and B. H. Crawford, Proc. R. Soc. London Ser. B **112,** 428 (1933).
13. G. Toraldo di Francia and L. Ronchi, J. Opt. Soc. Am. **42,** 782 (1952).
14. J. C. He, S. Marcos, and S. A. Burns, J. Opt. Soc. Am. A **16,** 2363 (1999).
15. A. Roorda and D. R. Williams, J. Vision **2,** 404 (2002).
16. B. Vohnsen, I. Iglesias, and P. Artal, Proc. SPIE **4964,** 24 (2003).
17. C. A. Curcio, K. R. Sloan, R. E. Kalina, and A. E. Hendrickson, J. Comp. Neurol. **292,** 497 (1990).
18. Laser Institute of America, "American National Standard for Safe Use of Lasers," Z136.1-2000 (Laser Institute of America, Orlando, Fla., 2000).
19. J. I. Yellot, Jr., Vision Res. **22,** 1205 (1982).